Theor Chem Acc (1999) 102:87–91
DOI 10.1007/s00214980m137

Theoretical
Chemistry Accounts

Regular article

Ab initio studies on the mechanism of dimerization reactions of ketene imine and bis(trifluoromethyl)ketene imine*

Xiaoyuan Fu, Yan Wang[1], Decai Fang

Department of Chemistry, Beijing Normal University, 100875 Beijing, People's Republic of China

Received: 15 July 1998 / Accepted 3 September 1998 / Published online: 17 December 1998

Abstract. The dimerization reactions of ketene imine and bis(trifluoromethyl)ketene imine were studied theoretically. All the dimerization processes take place in a concerted but asynchronous manner, each proceeding through a four-membered ring transition state. For the ketene imine dimerization reactions, three different processes have almost equal activation barriers, while for the three bis(trifluoromethyl)ketene imine dimerization processes the reaction giving symmetrical a four-membered heterocyclic product has the lowest activation barrier.

Key words: Ab initio calculation – Dimerization – Ketene imine – Bis(trifluoromethyl)ketene imine

1 Introduction

Ketene imines are known to dimerize [1–5] and trimerize [6] to yield heterocyclic compounds whose structures depend on the ketene imine substitution pattern and reaction condition. For example, Barker and Rosamond [2] reported that when diphenylketene *N*-methylimine is heated for 1 week at 125°C, the azetidine **1**, an unsymmetrical dimer results. Similar treatment of dimethylketene *N*-(2,6-dimethylphenyl)imine results in the production of the cyclobutane derivative **2** [3], whereas Deltsova et al. [4] have observed that bis(trifluoromethyl)ketene *N*-arylimines yield symmetrical heterocyclic dimers **3** when treated with "weak bases". To our knowledge, no theoretical studies have been reported on ketene imine dimerization reaction mechanisms. In this paper, we have used ketene imine and bis(trifluoromethyl)ketene imine as model compounds to study the reactions and the substituent effect theoretically. The reactions studied are as follows:

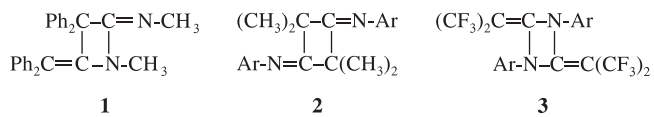

1 **2** **3**

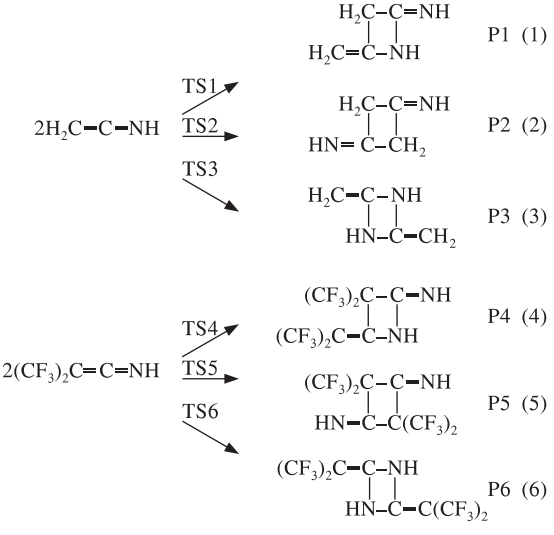

2 Methods of calculation

For the ketene imine dimerization reactions 1, 2 and 3, the geometries and energies of all the stationary points [reactants, transition states (TSs) and products] were fully optimized by means of the Berny method, a modified Schlegel method [7], with the RHF/6-31G and B3LYP/6-31++G** basis sets, while for the bis(trifluoromethyl)ketene imine dimerization reactions 4, 5 and 6, RHF/6-31G and B3LYP/6-31++G**//RHF/6–31G basis sets were used. Furthermore, all the TSs have been confirmed by vibrational analysis and characterized by the corresponding imaginary vibration modes and frequencies. All the calculations were carried out with the GAUSSIAN 94 program [8] on a Pentium Pro 200 computer.

The principal methods that has been used to study the electronic structure is Bader-type electron density

* Contribution to the Kenichi Fukui Memorial Issue

[1] *Present address*: Department of Chemistry, Xinyang Teachers College, 464000 Xinyang, Henan, China
Correspondence to: X. Fu

analysis [9–11]. Bond critical points are located by using Bader's topological analysis; it is suitable for seeing if cyclization took place or not. The topological properties of the electron density distribution of a molecule are based on the gradient vector field of the electron density $\nabla\rho(\mathbf{r})$, and on the Laplacian of the electron density $\nabla^2\rho(\mathbf{r})$, where $\mathbf{r}$ is a position vector of an electron in three-dimensional space.

The PC version of AIMPAC[12] was employed for the electron density topological analysis, using the electron densities obtained from the B3LYP/6-31++G** calculations with reactions 1–3.

3 Results and discussion

3.1 The dimerization reactions of ketene imine

The stationary points on the potential energy surface of the ketene imine dimerization reaction were located with the ab initio energy gradient method with RHF/6-31G and B3LYP/6-31++G** basis sets. For the three different dimerization routes 1, 2 and 3, one TS was found on each reaction path; therefore all three dimerization processes take place in an asynchronous concerted manner. The TSs located at the HF/6-31G and B3LYP/6-31++G** levels have only one imaginary vibration frequency each, corresponding to the motion along the reaction coordinate. The chief geometric parameters of the stationary points are given in Table 1. (For the configuration of the TS and atom numbering, see Fig. 1.) Inspection of the data in Table 1 reveals that all three dimerization processes are asynchronous and all the TSs have a twisted structure. This can be rationalized by the frontier molecular orbitals (FMOs) interaction of the reactants (see Fig. 2). For reaction 1, the interaction between the LUMO of one molecule and the HOMO of another one favors only the formation of a C—N bond, while,in reaction 2, the corresponding FMO interaction favors the formation of only one C—C bond; this accounts for the higher asynchronicity of reactions 1 and 2. However, reaction 3 favors the formation two C—N bonds of; therefore, reaction 3 has lower asynchronicity. This can be used to explain the differences between the dihedral angles of the four-membered ring TSs. Charges of 0.25*e*, 0.25*e* and 0.42*e* are transferred from one reactant to another in the TS for reactions 1, 2 and 3, respectively, stabilizing the TSs.

Topological properties of the TSs of the reactions are summarized in Table 2. Molecular graphs and Laplacian distributions of the TSs are shown in Fig. 3. In Fig. 3, positive values of $\nabla^2\rho_b$ are denoted by dashed lines and negative values by full lines. Bond paths (heavy solid lines), bond critical points (solid circle) and ring critical points (triangle) are shown for $\rho(\mathbf{r})$. For the three reactions, the C_4—C_1 bonds of reactions 1 and 2 have no bond paths and bond critical points in the corresponding TS; subsequently, TS1 and TS2 have no ring critical points. These results are consistent with the geometries. The C_4—C_1 bond and the four-membered ring are not formed in TS1 or TS2. They are formed only partially in TS3 which is less asynchronous than TS1 or TS2.

Table 1. The chief geometric parameters for the transition states (*TS*) and products (*P*) of the ketene imine dimerization reaction[a]

	HF/6-31G		B3LYP/6-31++G**	
	TS	P	TS	P
Reaction 1				
N_2—C_1	1.273	1.408	1.278	1.406
C_3—N_2	1.456	1.387	1.466	1.391
C_4—C_1	2.436	1.531	2.607	1.532
C_4—C_3	1.413	1.540	1.411	1.547
$\angle C_3N_2C_1$	112.79	95.60	115.97	95.57
$\angle C_4C_1N_2$	67.19	89.60	62.54	89.96
$\angle C_4C_1N_2C_3$	−20.54	0.00	−23.00	−0.02
Reaction 2				
C_2—C_1	1.404	1.521	1.388	1.530
C_3—C_2	1.768	1.531	1.741	1.539
C_4—C_1	3.248	1.531	2.817	1.539
C_4—C_3	1.345	1.521	1.375	1.530
$\angle C_3C_2C_1$	101.70	87.15	100.45	87.27
$\angle C_4C_1C_2$	48.72	92.85	63.53	92.73
$\angle C_4C_1C_2C_3$	30.38	0.02	28.33	0.03
Reaction 3				
C_2—N_1	1.345	1.415	1.338	1.424
N_3—C_2	1.465	1.415	1.454	1.424
C_4—N_1	2.161	1.415	2.144	1.424
C_4—N_3	1.279	1.415	1.292	1.424
$\angle N_3C_2N_1$	99.98	88.64	101.07	90.94
$\angle C_4N_1C_2$	75.86	91.37	76.19	89.05
$\angle C_4N_1C_2N_3$	8.41	0.05	4.46	0.01

[a] Bond lengths in angstroms, angles in degrees

The energies of all the stationary points (reactants TS and products) and the activation barriers of three dimerization routes are listed in Table 3. The result of B3LYP/6-31++G** shows that the three dimerization reactions, 1, 2 and 3, are competitive each other.

3.2 The dimerization reaction of bis(trifluoromethyl)ketene imine

For the three dimerization reactions of bis(trifluoromethyl)ketene imine, 4, 5 and 6, the geometries of

Fig. 1. The numbering system for the transition states (*TS*) of the ketene imine dimerization reaction

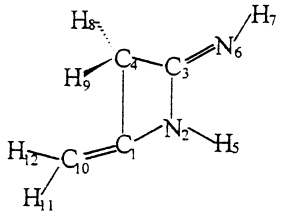

TS1

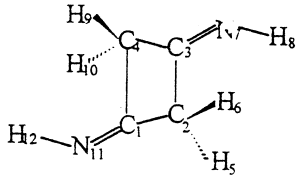

TS2

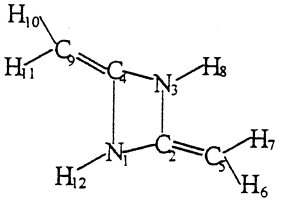

TS3

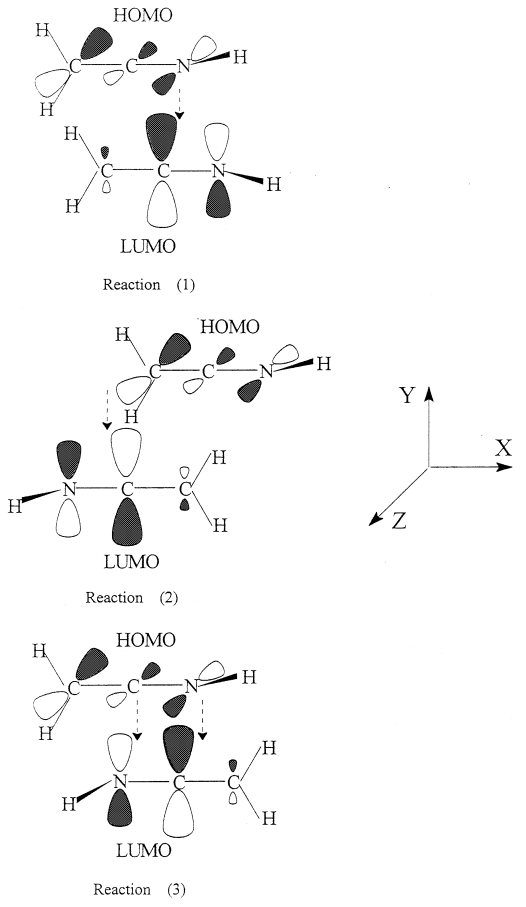

Fig. 2. The interaction of frontier molecular orbitals of reactions 1, 2 and 3 using B3LYP/6-31++G** results

Table 2. The topological properties of electron density distributions

Bond	ρ_b	$\nabla^2\rho_b$	ε	H_b
(1) TS1				
N2—C1	0.374	−0.711	0.138	−4.422
C3—N2	0.249	−0.630	0.061	−2.250
C4—C1				
C4—C3	0.303	−0.811	0.275	−2.036
N6—C3	0.382	−1.319	0.286	−4.278
C10—C1	0.344	−1.051	0.415	−3.130
(2) TS2				
C2—C1	0.299	−0.865	0.156	−2.428
C3—C2	0.150	−0.169	0.038	−0.582
C4—C1				
C4—C3	0.321	−0.901	0.338	−2.312
N7—C3	0.378	−1.119	0.198	−4.352
N11—C1	0.427	−0.357	0.133	−5.111
(3) TS3				
C2—N1	0.353	−1.231	0.227	−3.438
N3—C2	0.256	−0.643	0.022	−2.394
C4—N1	0.055	0.139	0.231	−0.025
C4—N3	0.370	−0.882	0.171	−4.275
C5—C2	0.326	−0.925	0.395	−2.438
C9—C4	0.347	−1.072	0.428	−3.260

►

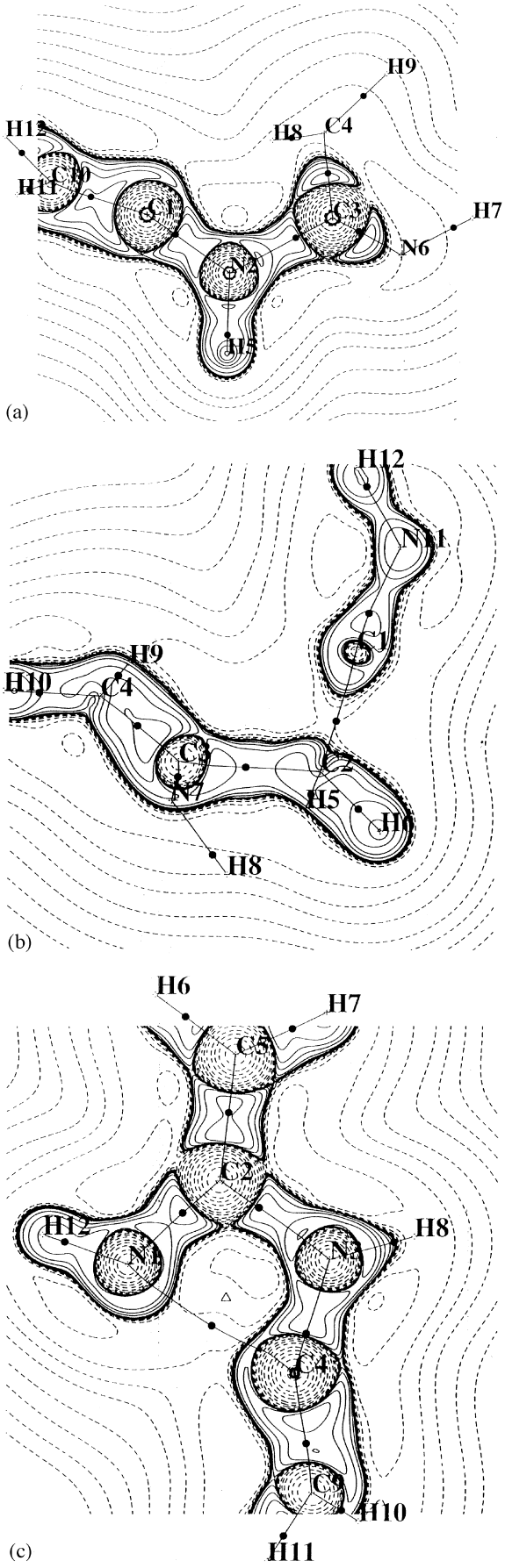

Fig. 3a–c. The molecular graphs and Laplacian distributions of the TSs for the dimerization reaction of ketene imine (according to the B3LYP/6-31++G** data). **a** TS1, **b** Ts2 and **c** TS3

stationary points were optimized only by using the HF/6–31G method owing to the complexity of this system. Similar to reactions 1–3, reactions 4–6 also proceed in an asynchronous concerted manner and each dimerization process has a twisted TS (see Fig. 4). The main geometric parameters of reactions are given in Table 4.

The calculated energy barriers at the HF/6-31G level of theory are 197.28, 220.99 and 173.28 kJ mol^{-1} respectively for reactions 4, 5 and 6. On account of the geometries of B3LYP/6-311++G** level is similar to that of HF/6-31G for reactions 1–3, single point B3LYP/6-311++G** calculations were carried out based on HF/6-31G geometries to improve the energies of reactions 4–6. The results give activation barriers of 136.55, 216.45 and 119.83 kJ mol^{-1} respectively for reactions 4, 5 and 6. The higher barrier of reaction 5 can be explained by steric hindrance effects. The nuclear repulsion energies for the TSs of reactions 4, 5 and 6 are 2237.02, 2310.99 and 2109.59 hartrees mol^{-1}, respectively, which show that the TS of reaction 5 has the highest steric hindrance effect. According to Mulliken population analysis, the CF_3 group in the reactant has only weak electron-releasing or electron-withdrawing effects; besides, the energy gap between the HOMO and the LUMO of bis(trifluoromethyl)ketene imine is nearly equal to that of ketene imine; therefore the electronic energies are similar for the two systems.

Table 3. The total energies of stationary points [reactants (*R*), TS and P] (E_h) and the activation barrier (kJ mol^{-1}) of the ketene imine dimerization reaction

	Total energy			Activation barrier
	R	TS	P	
HF/6-31G				
(1)	−263.62288	−263.54947	−263.68374	192.76
(2)		−263.54430	−263.67339	206.35
(3)		−263.55610	−263.66237	175.35
B3LYP/6-31++G**				
(1)	−265.45402	−265.40313	−265.50914	133.61
(2)		−265.40318	−265.49978	133.48
(3)		−265.40051	−265.48767	140.49

4 Conclusions

According to B3LYP/6-311**G** calculations, the following conclusions can be drawn from the results obtained.

1. The dimerization reactions of ketene imine and bis(trifluoromethyl)ketene imine are all concerted and asynchronous, taking place through twisted four-membered cyclic TSs.
2. For ketene imine dimerization reactions, the three different dimerization schemes have almost equal activation barriers, which shows that the three reactions compete with each other.
3. For the three bis(trifluoromethyl)ketene imine dimerization reactions, the process giving a symmetrical four-membered heterocyclic product has the lowest activation barrier, and these reactions are controlled by steric hindrance effects.

Acknowledgements. This project was supported by the National Nature Science Foundation of China (No. 29603002) and by the Foundation for Talented Youth Spanning the 20th Century of Beijing Normal University.

Table 4. The main geometric parameters for the TS and P of the (trifluoromethyl)ketene imine dimerization reaction[a]

Reaction (4)	TS	P	Reaction (5)	TS	P	Reaction (6)	TS	P
N_2—C_1	1.256	1.371	C_2—C_1	1.461	1.534	C_2—N_1	1.302	1.397
C_3—N_2	1.466	1.390	C_3—C_2	1.725	1.548	N_3—C_2	1.469	1.397
C_4—C_1	2.375	1.556	C_4—C_1	2.648	1.548	C_4—N_1	2.120	1.397
C_4—C_3	1.476	1.566	C_4—C_3	1.445	1.534	C_4—N_3	1.264	1.397
$\angle C_3N_2C_1$	114.04	97.49	$\angle C_3C_2C_1$	104.34	86.52	$\angle N_3C_2N_1$	100.61	89.33
$\angle C_4C_1N_2$	72.03	90.14	$\angle C_4C_1C_2$	73.48	93.48	$\angle C_4N_1C_2$	76.38	90.67
$\angle C_4C_1N_2C_3$	9.06	−0.87	$\angle C_4C_1C_2C_3$	−5.90	0.67	$\angle C_4N_1C_2N_3$	8.62	−0.01

[a] Bond lengths in angstroms, angles in degrees

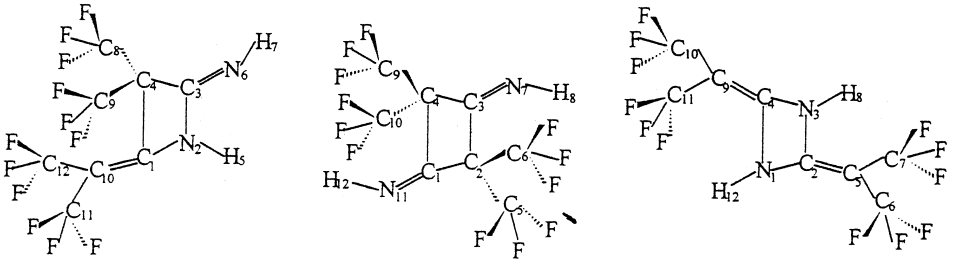

Fig. 4. The numbering system for TSs of the bis(trifluoromethyl)ketene imine dimerization reaction

TS4 TS5 TS6

References

1. Barker MW, Mchenry WE (1980) In: Patais (ed) The chemistry of ketenes, allenes and related compounds, part 2. Wiley, Chichester pp 702–720
2. Barker MW, Rosamond JD (1972) J. Heterocycl Chem 9:1147
3. Barker MW, Rosamond JD (1972) J. Heterocyclic Chem 11:241
4. Del'tsova DP, Gambaryan NP, Zeifman UyV, Knunyant IL (1972) Zh Org Khim 8:856
5. Fuks R, Baudoux D, Piccinni-Leopardi C, Declercq J-P, Meerssche MV (1988) J Org Chem 53:18
6. Barker MW, Rosamond JD (1973) J Heterocycl Chem 9:1419
7. Schegel HB (1982) J Comput Chem 3:214
8. Frisch MJ, Trucks GW, Schlegel HB, Gill PMW, Johnson BG, Robb MA, Cheeseman JR, Keith T, Petersson GA, Montgomery JA, Raghavachari K, Al-Laham MA, Zakrzewski VG, Ortiz JV, Foresman JB, Cioslowski J, Stefanov BB, Nanayakkara A, Challacombe M, Peng CY, Ayala PY, Chen W, Wong MW, Andres JL, Replogle ES, Gomperts R, Martin RL, Fox DJ, Binkley JS, Defrees DJ, Baker J, Stewart JP, Head-Gordon M, Gonzalez C, Pople JA (1995) GAUSSIAN 94. Gaussian, Pittsburgh, P
9. Bader RFW (1991) Chem Rev 91:893
10. Bader RFW (1990) Atoms in molecules: a quantum theory. Clarendon Press, Oxford
11. Bader RFW (1985) Acc Chem Res 18:9
12. AIMPAC is available from R.F.W. Bader's laboratory, McMaster University, Hamilton, Ontario, Canada. L8S 4M1; PC version was modified by De-Cai Fang and Ting-Hua Tang